



Study on the Applicability of " Five-Step Single Sidewall Guide Pit Method " for Loess Tunnels with Very Large Cross-Section

Minglei Qiao¹, Sheng Li^{1,*}, Yanjin Xue^{1,2}, Qicai Wang^{1,2}, Jiangong Zhang³ and Zhigang Chen¹

¹School of Civil Engineering, Lanzhou Jiaotong University, Lanzhou, Gansu, 730070, China

²State Local Joint Engineering Laboratory of Road and Bridge Engineering Disaster Prevention and Control Technology, Lanzhou Jiaotong University, Lanzhou, Gansu, 730070, China

³China Seventeen Metallurgical Group Co. Ltd. Maanshan, Anhui, 243000, China

*Corresponding author's e-mail: ligwin@126.com

Abstract. In order to strengthen the control ability of single sidewall guided pit method on surrounding rock deformation, and make it more suitable for the construction of very large section loess tunnel. The five-step single sidewall pit guide method is proposed by reserving core soil on the basis of single sidewall pit guide method. Taking the Fenghuang Mountain Tunnel of the expansion and renovation project of the Qingshuiyi-Zhonghe section of the G30 Lianhuo Expressway as the engineering background, the effects of changes in depth of burial, density, modulus of elasticity, cohesion and angle of internal friction on the settlement of the arch, horizontal convergence and stress of the steel arch frame were analyzed through numerical simulation, and the applicability of the five-step single sidewall pit guiding method was obtained: the density should not be more than 1.69g/cm^3 , and the modulus of elasticity should not be less than 50MPa.

Keywords: super large section; loess tunnel; five-step single sidewall guide pit method; numerical simulation; field test.

1 Introduction

With the implementation of the western development strategy, the economy of the northwest region, logistics and other rapid development, resulting in an unprecedented strong demand for transportation. The existing two-lane highway tunnel has been unable to meet the demand for transportation, so four lanes and more than the large section loess tunnel project is increasing [1], the construction of large section loess tunnel can not only meet the people's demand for transportation, but also to facilitate the neighboring provinces and regions of each other, and to promote the province's economic development is of great significance. Due to the large cross-section loess tunnels have the characteristics of large cross-section, large span and small flat rate, in order to ensure the construction safety, the construction method mostly adopts the double-sidewall

guided pit method or the single-sidewall guided pit method^[4]. Although the double sidewall guided pit method can be used for the excavation of very large section loess tunnel, it requires frequent erection and removal of temporary supports, which makes the construction speed slow and the construction cost high. Although the single sidewall guided pit method overcomes the above shortcomings, the control of surrounding rock deformation is not as good as the double sidewall guided pit method. Therefore, it is necessary to improve the single sidewall guided pit method, so that it can have the construction efficiency and better control of the surrounding rock deformation, which is more suitable for the construction of large cross-section loess tunnels.

Scholars at home and abroad have conducted researches on the construction methods of loess tunnels with very large sections. Soranzo et al^[2] studied the working face stability of shallow buried tunnels in partially saturated loess by centrifugal test and numerical analysis. Chambon et al^[3] systematically discussed the factors affecting the stability of the shallow tunnel face. The centrifugal model test was carried out on a shallow tunnel to study the limit value of the surrounding rock of the tunnel under various conditions. Regarding the double sidewall guided pit method, Yuan Long et al.^[4] utilized ANSYS software to numerically simulate different excavation support sequences of double sidewall guided pit method, and obtained the effects of different excavation support sequences on the deformation of surrounding rock in shallow buried large section loess tunnel, and gave the excavation support sequences that can control the deformation of surrounding rock on the surface and the deformation of surrounding rock in the tunnel. Jiang Ziliang^[5] Relying on the actual project, numerical simulation was used to optimize and determine the optimal spacing of the palisade faces for the double sidewall guide pit method of excavation, and the reasonableness of the spacing of the palisade faces was verified according to the construction monitoring data. Li Ming et al.^[6] Numerical simulation was used to compare and analyze the initial support force and deformation characteristics, surface settlement and pore water pressure field distribution characteristics of a water-rich large section loess tunnel constructed by double side-wall guided-pit method under the effect of fluid-solid coupling and no-coupling, which can be used as a guide for similar projects. Pan Chunyang et al.^[7] The distribution patterns of initial support rock pressure and grillage arch reinforcement stress in the construction section of double sidewall guided pit method were obtained by on-site monitoring method. Zhang Qinglin^[8] took the tunnel project of Xi'an Metro Line 6 as an example and used FLAC3D software to study in detail the deformation of the strata in the regional scope during the construction of the double sidewall guide pit method. Cao Qian et al^[9] used FLAC3D numerical calculation software to study the variation rules of stress and deformation in the surrounding rock of loess tunnels under different support strength conditions as well as the limit value of deformation for arch monitoring. Ruan et al^[10] compared the effects of different construction sequences of double-side heading method on surface settlement, surrounding rock stress and lining stress through indoor model tests. The experimental results show that compared with the upper and lower excavation methods, the surface settlement caused by the left and right excavation methods is smaller, the disturbance to the surrounding rock is smaller, and the stress of the supporting structure is more uniform and stable during the excavation process. Based on the actual project, Luo et al^[11] studied the space-time law of the

deformation of the surrounding rock supporting structure of the V-level shallow loess tunnel through numerical simulation and field monitoring. Regarding the single sidewall guided pit method, Fan Chuntan et al.^[12] Taking a loess tunnel as the background, numerical simulation of CRD method, CD method and three-step seven-step excavation method was carried out to analyze and compare the displacement, stress and elastic coefficient of reaction k of the surrounding rock under the three construction methods, and the numerical calculation results were examined by the measured data and the established theories, and the values of the elastic coefficient of reaction k of the different working methods were obtained. Luo Yanbin et al.^[13] The mechanical behavior of next door construction in the upper step CD method of mega-span tunnels is obtained by combining theoretical analysis, field testing and mechanical model calculation with the background of actual engineering. Li Bo et al.^[14] Relying on Zhengzhou-West Passenger Dedicated Line, the mechanical properties and deformation characteristics of different experimental methods, including single sidewall guide pit method, were obtained through on-site experimental tests and data analysis, and the applicability of different experimental methods was given for comprehensive evaluation. Zan Wenbo et al.^[15] used numerical simulation to systematically compare and analyze the four commonly used methods of large section loess tunnel excavation: three-step and seven-step excavation, middle and next door, cross middle and next door, and double side wall, and obtained the distribution law of perimeter rock deformation and perimeter rock pressure of different methods. Meng Xinzeng^[16] used finite element software to analyze the influence of locking anchor length, locking anchor laying angle and steel frame spacing on the deformation and support internal force of loess tunnel constructed by single sidewall guided pit method. Jin Jin^[17] used finite element software to study the deformation law of surrounding rock, stress distribution law and plastic zone distribution law of single sidewall guide pit method. In summary, domestic and foreign scholars have conducted a lot of research on the construction method of large section loess tunnel, but there are few studies on the optimization of the method for the single sidewall guide pit method.

Therefore, in order to strengthen the control ability of single sidewall guided pit method on surrounding rock deformation and make it more suitable for the construction of very large section loess tunnels, this paper proposes a five-step single sidewall guided pit method on the basis of single sidewall guided pit method, and takes the Fenghuangshan Tunnel of the expansion and renovation project of the Qingshuiyi-Zhonghe section of G30 Lianhuo Expressway as the engineering background. The effects of burial depth, density, modulus of elasticity, cohesion and change of internal friction angle on vault settlement, horizontal convergence and steel arch stress are analyzed by numerical simulation, and the applicability of the five-step single sidewall pit guide method is obtained.

2 Practical Engineering and Numerical Simulation

2.1 Summary of works

G30 Lianhuo Expressway Qingshuiyi to Zhonghe section expansion and renovation project Phoenix Hill Tunnel is located in Lanzhou City, Yuzhong County, for the separation of the double-hole long tunnel. Tunnel peripheral rock is mainly for the upper Pleistocene wind accumulation loess, its soil quality is more uniform, mainly powder, soil is drier, belongs to the V level peripheral rock. Measured by the field sampling, the highest water content of loess is 9.7%, cohesion and internal friction angle of up to 50.68kPa and 41.99 °, indicating that the tunnel loess surrounding rock quality is good. The length of Phoenix Hill Tunnel is 3945m, the maximum depth is 185m, the maximum excavation width of the tunnel is 17.89m, the maximum excavation height is 12.05m, and the excavation area is 182.5m², which belongs to the very large section loess tunnel^[18]. The tunnel adopts a five-step single sidewall guideway. The tunnel is constructed by five-step single sidewall guide pit method. The excavation footage is 1m, the second lining back arch is 6m each time, and the second lining of the cave body is 12m each time, and the support parameters are shown in Fig. 1.

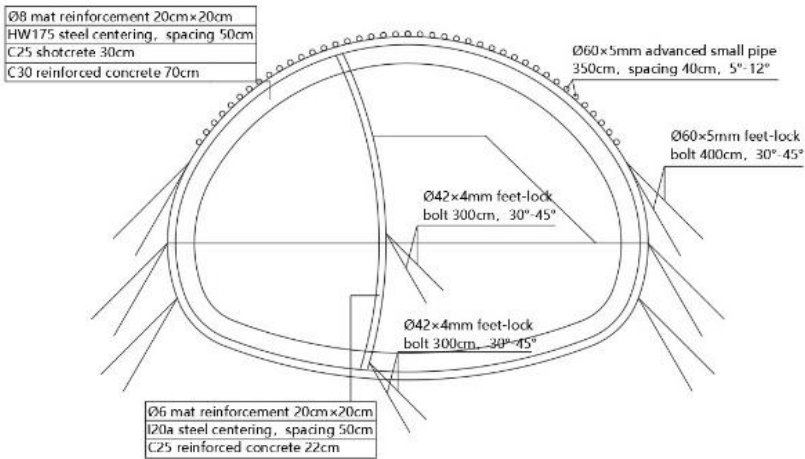


Fig. 1. Supporting parameters.

2.2 Introduction to the method

The five-step single sidewall guide pit method is optimized from the single sidewall guide pit method, and the difference between the two is:

(1) Location of the center wall. The location of the next door in the single sidewall guide pit method is located at half of the hole width, and the next door in the five-step single sidewall guide pit method is 0.45 times the hole width from the left excavation boundary.

(2) Whether to reserve core soil. The single sidewall guide pit method did not reserve core soil in the upper right guide pit, while the five-step single sidewall guide pit method reserved core soil with a width of 0.34 times the diameter of the hole and a height of 0.22 times the diameter of the hole for the purpose of controlling the problem of excessive settlement of the upper right guide pit section caused by the leftward movement of the center wall.

A comparison of the single sidewall guided pit method with the five-step single sidewall guided pit method is shown in Figure 2.

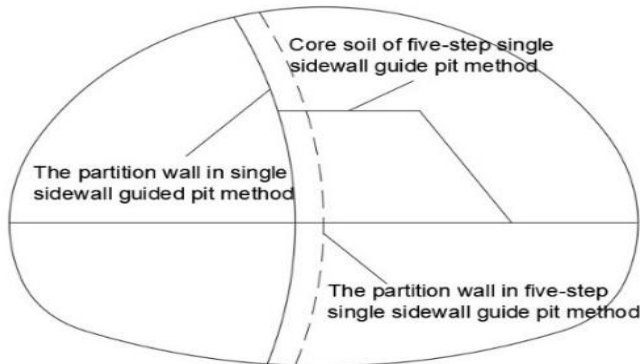


Fig. 2. Comparison of single sidewall guide pit method and five-step single sidewall guide pit method.

2.3 Modeling

2.3.1 Modeling methodology.

In this paper, numerical simulation of five-step single sidewall guide pit method is carried out. Currently, there are two methods on tunnel modeling, one is the life and death unit method and the other is the tracking unit method^[19] The other is the tracking unit method. The life and death unit method is to connect the soil body with the lining through the contact relationship, and using the life and death unit function, the lining will be activated at the original position after killing the soil body in the tunnel excavation area, so as to realize the simulation of tunnel excavation and support. The tracking unit method has only one component, the soil body, by modifying the model file, the soil body and the lining of the overlap of the unit copied to generate the lining, these copied units and the copied unit common node, so that the lining can track the deformation of the soil body, and thus activated in the deformation of the soil body position, so that the simulation is more in line with the actual construction process, and the tracking unit method has a fast computation speed, easy to convergence, and so the tracking unit method is used in this paper. Therefore, this paper adopts the tracking unit method for modeling, and Figure 3 shows the modeling flow of the two methods.

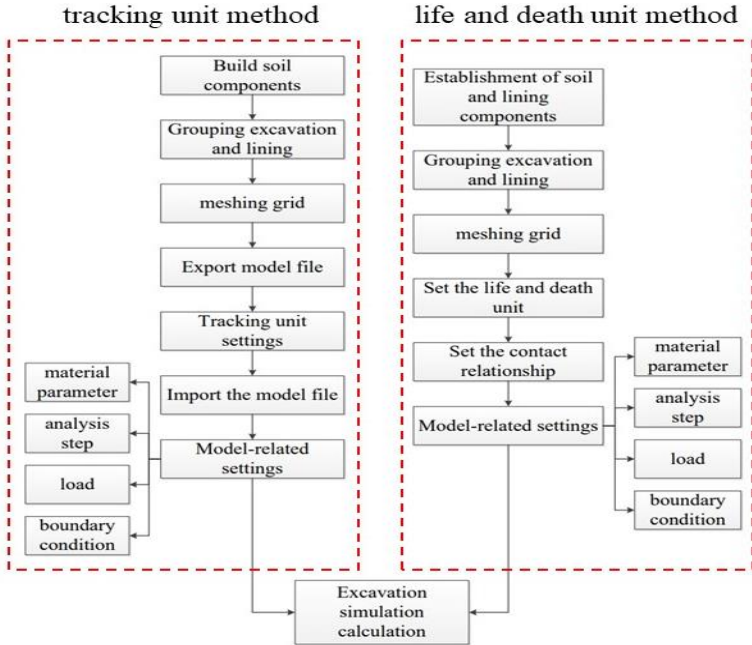


Fig. 3. Modeling process.

According to the principle of St. Venant, the scope of tunnel excavation disturbance zone is generally 3-5 times the diameter of the hole, so the model is 138m wide, 133m high (buried depth of 60m), the longitudinal length of 60m, the model schematic diagram is shown in Figure 4. In the excavation process setup, the excavation feed is 1m, the second lining back arch is laid 6m each time, the second lining cave body is laid 12m each time. The excavation sequence of five-step single sidewall guide pit method is in the order of the left upper guide pit, left lower guide pit, right upper guide pit, core soil and right lower guide pit, and the length of the steps is 5m.

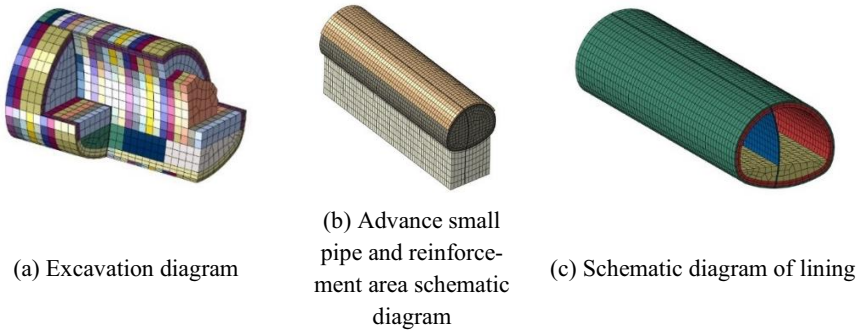


Fig. 4. Schematic diagram of finite element calculation model.

2.3.2 Modeling parameters.

The surrounding rock of the model is modeled by Mohr-Coulomb intrinsic model, the primary liner and the secondary liner are simulated by solid unit C3D8R, the steel arch of the primary liner is embedded in shotcrete by using built-in commands, and the steel arch and anchors are simulated by beam unit. In order to simplify the calculation, the overrun small conduit and the base rotary spray pile are simulated according to the principle of equivalent stiffness.^{[20][21]} and the second liner and steel reinforcement are considered as a whole.^[22] The second liner and reinforcement are considered as a whole. The release of surrounding rock stress during excavation is considered by the method of reducing the modulus of elasticity of soil in the excavation area.^[23] The method of reducing the modulus of elasticity of the soil in the excavation area was used. After combining the indoor test and referring to the "Road Tunnel Design Code" (JTG 3370.1-2018)^[24], the numerical simulation parameters are shown in Table 1. After that, the numerical simulation parameters are shown in Table 1.

Table 1. Numerical simulation parameters.

	gravity /(N/m ³)	elastic modulus /(MPa)	pois- son ra- tio	cohesion /kPa	angle of inter- nal friction /(°)
Aeolian loess	15700	80	0.4	35	29
shotcrete	22000	26000	0.2		
secondary liner	25000	35000	0.2		
steel centering	78500	210000	0.2		
feet-lock bolt	78500	210000	0.3		
Advanced small pipe reinforce- ment area	18840	463	0.3	42	35
Reinforcement area of jet grouting pile	20410	1000	0.3	45	37

3 Analysis of the applicability of the five-step single sidewall guide pit method

In this chapter, the effects of burial depth, density, modulus of elasticity, cohesion and internal friction angle changes on the settlement of the vault, horizontal convergence and maximum stress of the steel arch in a section are analyzed by numerical simulation, and the applicability of the five-step single-sidewall guided pit method is analyzed in this way. According to the "Highway Tunnel Design Code" (JTG 3370.1-2018), combined with the actual size of the tunnel in this project, the deep and shallow burial limit of Phoenix Hill Tunnel is obtained as 34.38m, and the shallow burial of 20m and 30m, and the deep burial of 40m and 60m are taken as the burial depth of the tunnel for numerical simulation, and the parameters of the numerical simulation are set up as described in section 2.3.2

3.1 Density changes at different burial depths

The modulus of elasticity, cohesion and angle of internal friction of the model are set according to Table 1, and the density is calculated from 1.57g/cm³ to 1.69g/cm³ during the change of density, the change rule of the steel arch stress, the settlement of the vault and the horizontal convergence of the steel arch with different depth of burial, and the results of the calculations are shown in Fig. 5. As can be seen from the figure, for the steel arch stress, when the depth of burial is unchanged, with the gradual increase in density, the steel arch stress is gradually increasing. When the density is unchanged, with the increase of burial depth, the steel arch stress also increases gradually. For the arch settlement and horizontal convergence, with the gradual increase of burial depth, the arch settlement and horizontal convergence also gradually increase with the increase of density, and different depths of burial, the magnitude of the increase of the two is different, when the depth of burial is shallow, the magnitude of the change of the two is small, and when the depth of burial is large, the increase of the two is large. Among them, when the burial depth is 60m and the density is 1.69g/cm³, the arch settlement and horizontal convergence reach the maximum value, which is 11.09cm and 7.12cm, respectively, and the maximum steel arch stress is 191.3MPa, and the steel arch stress has exceeded the specification requirements. Meanwhile, combining with Fig. 5(a) and Technical Specification for Highway Tunnel Construction (JTGT3660-2020)^[25], it can be obtained that the maximum density of the five-step single sidewall guide pit method can not exceed 1.68g/cm³ when the burial depth is 60.

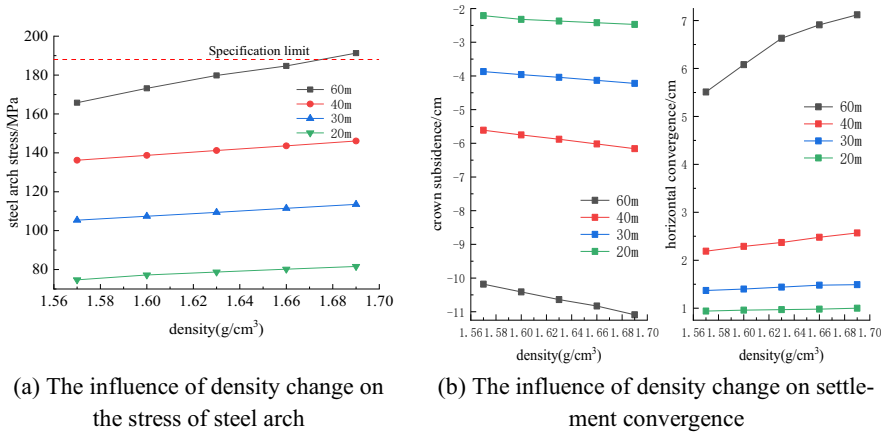
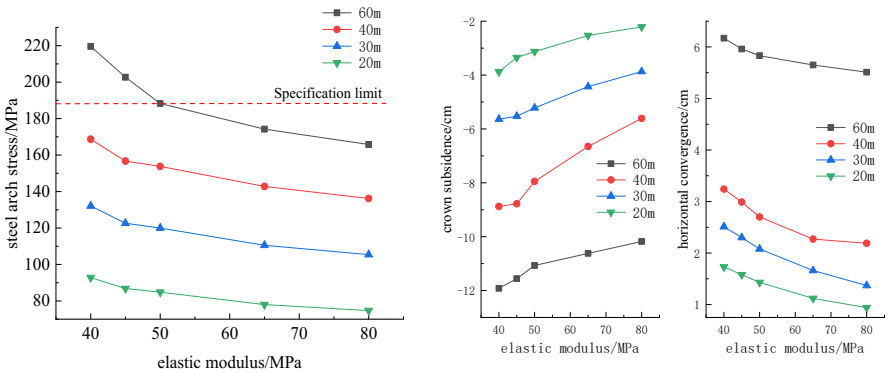


Fig. 5. Effect of density on stress and settlement convergence of steel arch.

3.2 Variation of elastic modulus at different burial depths

The density, cohesion and angle of internal friction of the model are set according to Table 1, and the change rule of steel arch stress, arch settlement and horizontal convergence in different burial depths is calculated during the change of modulus of elasticity from 40MPa to 80MPa, and the results are shown in Fig. 6. As can be seen from the

figure, when the burial depth is unchanged, with the gradual increase of elastic modulus, the steel arch stress, vault settlement and horizontal convergence are gradually reduced. When the modulus of elasticity is unchanged, with the increase of burial depth, the steel arch stress, vault settlement and horizontal convergence also increase gradually. Among them, when the burial depth is 60m and the modulus of elasticity is 40MPa, the arch settlement and horizontal convergence reach the maximum value, which is 11.92cm and 6.17cm, respectively, and the steel arch stress is 219.6MPa, which exceeds the specification requirements. Meanwhile, combining with Fig. 6(a) and Technical Code for Highway Tunnel Construction (JTGT3660-2020), it can be obtained that the maximum modulus of elasticity of five-step single-sidewall guided pit method can not be less than 50MPa when the burial depth is 60m.



(a) The influence of elastic modulus change on the stress of steel arch

(b) The influence of elastic modulus change on settlement convergence

Fig. 6. Effect of elastic modulus on stress and settlement convergence of steel arch.

3.3 Variation of cohesion at different burial depths

The density, modulus of elasticity and angle of internal friction of the model are set according to Table 1, and the change rule of steel arch stress, vault settlement and horizontal convergence for different burial depths is calculated during the change of cohesion from 20kPa to 45kPa, and the calculation results are shown in Figure 7. As can be seen from the figure, for the steel arch stress, although the greater the depth of burial, the greater the steel arch stress, but when the depth of burial is unchanged, with the increase of cohesion, the steel arch stress is almost unchanged, which shows that the change of cohesion can't have an effect on the steel arch stress. For the vault settlement and horizontal convergence, when the cohesive force is constant, with the depth of burial gradually increasing, the vault settlement and horizontal convergence also gradually increase, when the depth of burial is constant, the vault settlement and horizontal convergence decrease with the increase of cohesive force. And, the magnitude of the decrease of both increases with the increase of burial depth, when the cohesive force increases to a certain critical value, the arch settlement and horizontal convergence of the

various burial depths basically no longer change, and this critical value increases with the increase of burial depth. For example, when the burial depth is 30m, the cohesive force is greater than the critical value of 30kPa, the vault settlement in the horizontal convergence will basically no change, and when the burial depth is 40m, the cohesive force is greater than the critical value of 40kPa, the vault settlement in the horizontal convergence will basically no change.

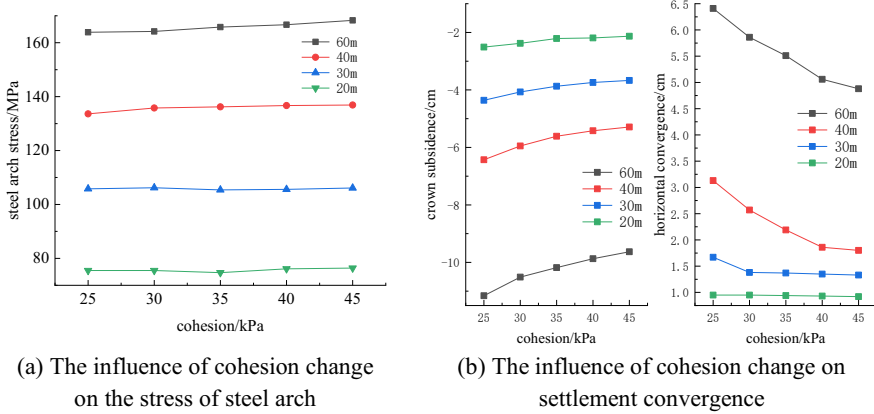


Fig. 7. Effect of cohesion on stress and settlement convergence of steel arch.

3.4 Variation of internal friction angle at different burial depths

The density, modulus of elasticity and cohesion of the model are set according to Table 1, and the change rule of steel arch stress, vault settlement and horizontal convergence for different burial depths is calculated during the change of internal friction angle from 23° to 35°, and the calculation results are shown in Fig. 8. As can be seen from the figure, for the steel arch stress, when the depth of burial is unchanged, as the internal friction angle gradually increases, the steel arch stress is gradually increasing. When the angle of internal friction is unchanged, with the increase of burial depth, the steel arch stress is also gradually increased. For vault settlement and horizontal convergence, when the angle of internal friction is constant, with the gradual increase of burial depth, the vault settlement and horizontal convergence also increase gradually, and when the burial depth is constant, the vault settlement and horizontal convergence decrease with the increase of the angle of internal friction. And, the magnitude of the two decreases with the increase of the depth of burial increases, when the internal friction angle increases to a certain critical value, the arch settlement and horizontal convergence of the various burial depths basically no longer change, and this critical value increases with the increase of the depth of burial. For example, when the burial depth is 30m, after the internal friction angle is greater than the critical value of 29°, the vault settlement in the horizontal convergence is basically unchanged, while the burial depth is 40m, the internal friction angle is greater than the critical value of 32°, the vault settlement in the horizontal convergence is basically unchanged.

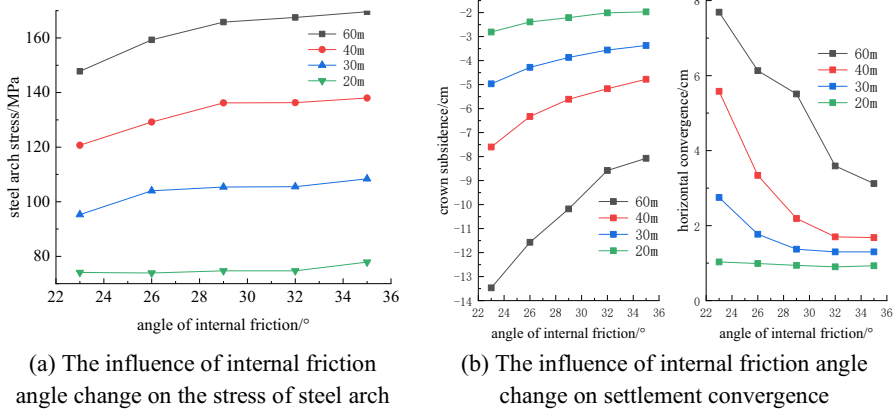


Fig. 8. Effect of internal friction angle on stress and settlement convergence of steel arch.

Through the above analysis, it can be found that, with the increase of cohesion and internal friction angle, the settlement and horizontal convergence of the arch are reduced, and the reduction increases with the increase of burial depth, and has a critical value, but the change of cohesion and internal friction angle is not obvious to the steel arch stress, and when the burial depth is increased, the steel arch stress does not exceed the specification limit, so the cohesion and the angle of friction can't be taken as a five-step single-sidewall guided pit method. Applicability index. When the density is bigger, the elastic modulus is smaller, and the burial depth is bigger, the steel arch stress, arch settlement and horizontal convergence are bigger, when the burial depth is 60m, the density is more than 1.69g/cm^3 , and the elastic modulus is less than 50MPa, according to the "Technical Specification for Highway Tunnel Construction" (JTGT3660-2020), the five-step single-sidewall guided pit method can't be used.

4 Conclusion

In this paper, the applicability of the five-step single sidewall guide pit method is analyzed by numerical simulation and the following conclusions are obtained:

(1) When the density of loess is higher, the modulus of elasticity is lower, and the depth of burial is greater, the steel arch stress, arch settlement and horizontal convergence will be greater.

(2) When the cohesion and internal friction angle increase, the settlement and horizontal convergence of the arch are reduced, and the reduction increases with the depth of burial, and has a critical value, and the critical value increases with the depth of burial. When the cohesion and internal friction angle change, the change of steel arch stress is not obvious.

(3) Five-step single sidewall guide pit method applicable conditions: density should not exceed 1.69g/cm^3 , modulus of elasticity should not be less than 50MPa, The results of this study can be used as a reference for future similar projects when using the five-step single sidewall guide pit method.

(4) The five-step single sidewall guided pit method, compared with the double sidewall guided pit method, takes into account the construction efficiency while controlling the deformation of the surrounding rock, which is of great significance to shorten the construction period and save the construction cost.

Acknowledgments

The authors would like to acknowledge the financial support provided by the National Science Foundation of China(51868041), the Basic Research Innovation Group Project of Gansu Province (21JR7RA347),the National Science Foundation of Gansu Province(22JR5RA338),the Key R & D Program Funding of Ningxia(2022BEG02056).

References

1. ZHANG J R, WU J, YAN C W, et al. (2020) Construction Technology of Super-large Section of Highway Tunnels with Four or More Lanes in China[J].China Journal of Highway and Transport ,33(01):14-31.
2. E. Soranzo, R. Tamagnini, and W. Wu. Face stability of shallow tunnels in partially saturated soil: centrifuge testing and numerical analysis. *Géotechnique* 2015 65:6, 454-467.
3. Chamborn P, Cort'e J F. Shallow tunnels in cohesionless soil. Stability of tunnel face[J].ASCE Journal of Geotechnical Engineering,1994,120:1148-1165.
4. YUAN L, HE W S. (2022) Study on the Application of Double-Side Heading Method in the Construction of Shallow and Large Section Loess Tunnel[J]. Journal of Underground Space and Engineering, 18(S1):289-295.
5. JIANG Z L. (2022) Construction Parameters Optimization for Double-sidewalls Guiding-hole Method of Shallow Buried Urban Subway Tunnel in Loess Formation [J]. Rail-way Engineering ,62(03):126-131.
6. LI M, YAN S H, PAN C Y, et al. (2019) Analysis of Fluid-Solid Coupling Effect during Excavation of the Water-rich Large-section Loess Tunnel [J]. Modern Tunnelling Technology ,56(04):81-88.
7. PAN C Y, YAN S H, LIANG X, et al. (2017) Mechanical Analysis of Lattice Arch Used in Large Span Running Tunnel in Loess Stratum by New Austrian Tunneling Method [J]. Railway Engineering, (02):60-63.
8. ZHANG Q L. (2023) Analysis of the influence of large section excavation of double side heading method on stratum deformation in loess stratum[J]. Sichuan Cement, (03):175-177.
9. CAO Q, CHEN J, SUN C C, et al. (2022) Mechanical Properties and Deformation Limit Value of Surrounding Rocks in Loess Tunnel Construction by Double-side Heading Method[J]. Journal of Hydraulic and Architectural Engineering, 20(02):59-65.
10. Ruan, Y.; Luo, X.; Li, J.; Li, Y.; Lin, S.; Ling, C.; Yuan, B. Deformation Law of Tunnels Using Double-Sidewall Guide Pit Method under Different Excavation Sequences. *Appl. Sci.* 2023, 13, 12764.
11. Luo Y, Chen J, Shi Z, et al. Mechanical characteristics of primary support of large span loess highway tunnel: a case study in Shaanxi Province, Loess Plateau, NW China primary[J]. *Tunnelling and Underground Space Technology*, 2020, 104: 103532.

12. FAN C T, LIANG Q G, FANG Z Q, et al. (2022) Influence of Construction Method on Interaction of Surrounding Rock Structure of Loess Tunnel[J]. Journal of Railway Engineering Society ,39(11):81-87.
13. LUO Y B, SHI Z, CHEN J X, et al. (2020) Mechanical Calculation Model and Research on Construction Mechanical Behavior of Middle Diaphragm in Upper Bench CD Method for Super-large Span Tunnel[J]. China Journal of Highway and Transport ,33(12):235-248.
14. LI B, SONG Z, SHI Y L, et al. (2015) Study on Mechanical and Deformation Characteristics of Large Cross-section Loess Tunnels Constructed by Different Methods [J]. Tunnel Construction ,35(06):508-513.
15. ZAN W B, LAI J X, QIU J L, et al. (2017) Numerical Analysis on Excavation Scheme for Four-lane Large-span Shallow-buried Loess Tunnel[J]. Journal of PLA University of Technology (Natural Science Edition) ,18(01):36-42.
16. MENG X Z. (2018) Research on the simulation of the excavation deformation and the internal force of support structure in loess tunnel[D], Chang'an University.
17. JIN J. (2017) The Research for Large Cross-section Loess Tunnel Excavation Deformation Monitoring and Analysis of the Construction Process[D], Lanzhou Jiaotong University.
18. ZHAO Y. (2011) Loess Tunnel Project[M]. Beijing: China Railway Press,Beijing.
19. DU W M. (2014) Reserch on Excevate and Support Method Optimization in Large Cross-Section of Gas Tunnel by Numerical Simulation[D].Chengdu:Southwest Jiaotong Univer-sity.
20. LI S C, CHEN H B,ZHANG C,et al. (2017) Research on effect of advanced support in silty clay tunnel[J].Rock and Soil Mechanics ,38(S2):287-294.
21. LAI J X, FAN H B, XIE Y L,et al. (2016) Consolidation Analysis of Jet Grouting Pile Re-inforcement in Loess Tunnel[J].Journal of Chang’an University(Natural Science Edition) ,36(02):73-79.
22. YIN M L, ZHANG J X, JIANG Y S, et al. (2021) Optimal Length of Transition Section in Super-large Cross-section Tunnel [J]. Science Technology and Engineering ,21(03):1163-1168.
23. FEI K, ZHANG J W. (2010) Application of ABAQUS in Geotechnical Engineering[M]. Beijing:China Water Resources and Hydropower Press.
24. Ministry of Transport of the People's Republic of China. Speifications for Design of Highway Tunnels: JTG 3370.1-2018[S].Beijing: China Communications Press,2018.
25. Ministry of Transport of the People's Republic of China. Highway geotechnical test procedures: JTG 3660-2020[S].Beijing: China Communications Press,2020.

Open Access This chapter is licensed under the terms of the Creative Commons Attribution-NonCommercial 4.0 International License (<http://creativecommons.org/licenses/by-nc/4.0/>), which permits any noncommercial use, sharing, adaptation, distribution and reproduction in any medium or format, as long as you give appropriate credit to the original author(s) and the source, provide a link to the Creative Commons license and indicate if changes were made.

The images or other third party material in this chapter are included in the chapter's Creative Commons license, unless indicated otherwise in a credit line to the material. If material is not included in the chapter's Creative Commons license and your intended use is not permitted by statutory regulation or exceeds the permitted use, you will need to obtain permission directly from the copyright holder.

